Internal structure dependent creep motion of domain walls driven by spin-transfer torques

Lucas Javier Albornoz,[1,2,3,4] Rebeca Díaz Pardo [1,5] Aristide Lemaître,[6] Sebastian Bustingorry [3,4]
Javier Curiale [2,3,4] and Vincent Jeudy [1]

[1]*Laboratoire de Physique des Solides, Université Paris-Saclay*, CNRS, 91405 Orsay, France
[2]*Instituto Balseiro, Univ. Nac. Cuyo - CNEA*, Av. Bustillo 9500 (R8402AGP), S. C. de Bariloche, Río Negro, Argentina
[3]*Instituto de Nanociencia y Nanotecnología (CNEA-CONICET)*, Nodo Bariloche, Av. Bustillo 9500 (R8402AGP),
S. C. de Bariloche, Río Negro, Argentina
[4]*Gerencia de Física, Centro Atómico Bariloche*, Av. Bustillo 9500 (R8402AGP), S. C. de Bariloche, Río Negro, Argentina
[5]*Departamento de Estado Sólido, Instituto de Física, Universidad Nacional Autónoma de México*,
Apartado Postal 20-364, Ciudad de México C.P. 01000, Mexico
[6]*Centre de Nanosciences et et Nanotechnologies (C2N)*, CNRS, *Université Paris-Saclay*, 91120 Palaiseau, France

We explore the contributions of adiabatic and nonadiabatic spin-transfer torques (STT) of a spin-polarized current to the thermally activated creep motion of domain walls in a thin (Ga,Mn)(As,P) film with perpendicular anisotropy. The nonadiabatic STT is found to compensate linearly an external magnetic field, with a slope compatible with a steady domain-wall internal structure. Close to the compensation, the adiabatic contribution is strongly enhanced and may both increase or reduce domain-wall velocity, which we associate to variations of creep pinning energy barrier with domain-wall internal structure. Far from compensation, the effects of adiabatic STT become negligible and so field and current driven domain-wall motion presents common universal behaviors described by the quenched Edwards Wilkinson universality class.

I. INTRODUCTION

The dynamics of magnetic domain walls (DWs) driven by spin polarized electrical current have been the subject of a large amount of fundamental and applied research in the past decades due to expected applications to spintronic devices [1,2]. When a current is crossing a DW, the spin transfer from charge carriers to the local magnetic moments of atoms may be phenomenologically described by adiabatic and nonadiabatic contributions [3,4]. The dynamics of DW results from the coupling between its velocity and internal magnetization precession frequency. In thin films with perpendicular anisotropy, for a DW transverse to current, the nonadiabatic torque (na-STT) is equivalent to a perpendicular magnetic field, and controls the velocity, while the precession of DW internal magnetization depends both on adiabatic spin-transfer torque (a-STT) and na-STT. A so-called Walker threshold is expected to separate DW motion with a steady magnetic structure at low drive from that with a precessional structure at high drive [5]. In the presence of disorder inherent to magnetic materials, the pinning strongly modifies DW dynamics. Despite a fairly abundant theoretical [6–8] and experimental [9–14] literature on this topic, the respective contributions of a-STT and na-STT to DW depinning and dynamical behaviors remain an open issue.

The competition between DW interaction with random disorder, its elasticity, the driving force f (associated to field or current), and thermal noise leads to rich universal behaviors [14–16], shared by a large variety of interfaces moving in random media [17]. Below a depinning threshold, DWs move in the thermally activated creep regime. The velocity scales as

$\ln v \sim f^{-\mu}$, where μ is the universal creep exponent. Field driven DW motion in thin ferro- and ferrimagnets [18,19] is well described by the value $\mu = 1/4$ [16,20]. This value coincides with prediction for a one-dimension elastic line, with short range elasticity and disorder interactions, moving in a two-dimensional medium [15] described by the so-called quenched Edwards Wilkinson universality class [21]. Current driven DW motion presents slightly different universal behaviors. In extended geometry, the DWs are observed to form mountainlike structures [12,14], which reflects the directionality of current-DW interaction causing a decrease of the drive-magnitude with increasing DW tilting [14]. However, for DWs kept transverse to current, magnetic field and current driven DW motion were found to present common creep [11,14] and depinning universal behaviors [14]. Note that, in tracks, the tilting of DWs [9,13], Joule heating [11,22–24], and the contribution of edge pinning as revealed by domelike DW shapes [13,25] may lead to effective creep exponents different from the universal value $\mu = 1/4$.

In this context, the respective contributions of the STTs to creep motion remain controversial. Duine and Morais Smith [6] and later Ryu *et al.* [7] suggested that a key ingredient in addition to DW elasticity could be its magnetic texture. In their model, developed for a DW transverse to current, the pinning potential depends both on the DW position and its internal magnetization tilting angle. They predict that the na-STT is equivalent to a magnetic field as for free DW motion [4]. Surprisingly, for the contribution of a-STT to DW magnetization tilt, both Refs. [6,7] neglect the DW Bloch/Néel anisotropy, which favors a magnetization

direction parallel to DW, and only consider [7] its spatial fluctuations due to disorder. The contribution of a-STT is also assumed to enhance DW pinning [6,7], while it could be at the origin of nontrivial creep dynamical behaviors [26]. On the experimental side, a proportionality relation between the torques exerted by na-STT and magnetic field has not yet been established, even if their equivalence seems rather well accepted [10,11]. Moreover, determining the contribution of a-STT to DW creep motion remains an experimental challenge due to Joule heating which may vary significantly the sample temperature [11,23,24] and impedes stringent tests of theoretical predictions.

Here, we report a study on DW creep motion in an extended geometry and for which Joule effects are precisely avoided. We enlighten a compensation between magnetic field and na-STT over one order of magnitude of current density, which is compatible with a frozen direction of DW magnetization. Close to the compensation, the contribution of a-STT is found to increase and also reduce DW velocity, which rules out a contribution of a-STT only dominated by DW pinning. The model of energy barrier that we develop to account for experimental observations relies on combined contributions of magnetic field, na-STT, and a-STT to DW motion and magnetic texture. Section II presents the experimental methods and a phenomenological description of DW motion. In Sec. III, we discuss the zero crossing of DW velocity and analyze the contribution of nonadiabatic STT. Section IV is dedicated to the role played by adiabatic STT on the DW magnetic texture and creep motion.

II. PHENOMENOLOGY OF DOMAIN-WALL MOTION

A. Experimental methods

The DW motion was studied in a 4 nm thick film of a diluted magnetic semiconductor forming part of a stack made of AlAs(30)/GaAs(2)/(Ga,Mn)(As,P)(3)/(Ga,Mn)As(1) (the numbers in parentheses are the thicknesses in nm), grown by molecular beam epitaxy on a (001) GaAs/AlAs buffer [27]. The film has a perpendicular anisotropy and a Curie temperature $T_C = 65$ K. It was patterned by electron lithography into a rectangle shape of size 133×210 μm². Two 40 μm wide gold electrodes separated by 110 μm were deposited by evaporation parallel to the narrow sides of the rectangle. They were used to generate a homogeneous current density producing DW motion by STT (see [14] for details). The current pulse amplitude varied between 0 and 11 GA/m². We verified that the Joule effect had a negligible contribution on DW dynamics, as reported in details in Ref. [14] and expected for a sample ten times thinner than the one previously used (~50 μm) [5,28,29]. Perpendicular magnetic field pulses of adjustable amplitude (0–65 mT) were produced by an ≈75 turns small coil (diameter ≈ 1 mm; rise time $\tau \approx 100$ ns) mounted on the sample. The sample was fixed in an optical He-flow cryostat allowing a temperature regulation between 5.7 K and T_C. To observe the dynamics of the DWs, we used a magneto-optical Kerr effect microscope in polar configuration (resolution ~1 μm). The mean displacement of DWs (Δx) was produced by magnetic field and/or current pulses of duration (Δt), which could be adjusted between 1 μs and 120 s in

order to measure significant DW displacements ($\Delta x \approx 10$ μm) with $\Delta t \gg \tau$. The DW velocities are defined as the ratio $v = \Delta x / \Delta t$. The phenomenology of domain-wall motion is described in Fig. 1, for a temperature $T = 55$ K.

B. Universal creep dynamics

Independent magnetic field and current driven DW motion is compared in Fig. 1(g). As can be observed, both velocity curves, $v(H, J = 0)$ and $v(H = 0, J)$, present a good agreement with the creep scaling law $\ln v \sim H^{-\mu}$, and $\ln v \sim J^{-\mu}$, with the same value for the creep exponent ($\mu = 1/4$). For the current, the good scaling with a constant temperature is a signature of negligible contribution of the Joule heating effect. Note that, as already demonstrated in Ref. [14], the additional higher order J term proposed in Ref. [11] is not necessary to account for experimental data. Therefore, the DW dynamics are compatible with common universal behavior, as discussed in details in Ref. [14]. Note that the two curves (for which $\mu_0 H^{-\mu}$ and $J^{-\mu}$ share the same scaling) cross so that a simple homothety between $\mu_0 H$ and J is not sufficient to superimpose them, as assumed in previous works [10,11]. The observed slightly different slopes originate from the different material dependent pinning parameters controlling field and current driven DW motion [14].

C. Combined current and field driven dynamics

The motion of DWs produced by combined current and magnetic field pulses (of the same duration) are reported in Figs. 1(a)–1(c). The initial state [see Fig. 1(a)] consists of two parallel DWs (called left and right DW in the following) separating a central domain with magnetization $\vec{M}$ perpendicular to the film and two domains with opposite magnetization directions. A combined current and magnetic field pulse pushes differently the two DWs [see Fig. 1(b)]. The current moves the two DWs in the same direction, opposite to the current flow (towards the right side), as expected for (Ga,Mn)As [5,10], while the magnetic field changes the distance between the two DWs (the central domain width is reduced due to the opposite direction between magnetic field $\vec{H}$ and magnetization $\vec{M}$). As a result [see Fig. 1(c)], the mean displacement of the left (Δx_L) [right (Δx_R)] DW is larger (smaller) due to the additive (opposite) contributions of current and field.

D. Zero crossing of domain-wall velocity

More insights into dynamics are shown in Fig. 1(e), which compares the left and right DW velocities ($v_{L,R} = \Delta x_{L,R}/\Delta t$) versus current density (J). As expected, the additive (subtractive) contributions of the field and current enhance (reduce) the velocity of left [$v_L(J, H)$] (right [$v_R(J, H)$]) DW compared to the zero field velocity $v(J, 0)$. Interestingly, as the current density is reduced, the velocity v_R is observed to go to zero (for $J \approx 4$ GA/m²) and to change of sign. Highlights of this phenomenon are reported in Fig. 1(f), which shows the absolute value of v_R in semilog scale versus J for different fixed applied magnetic fields. As it can be observed, the value of current density (J_c) at which the compensation occurs systematically increases with increasing applied magnetic field value. Notice also that the velocity curves present an
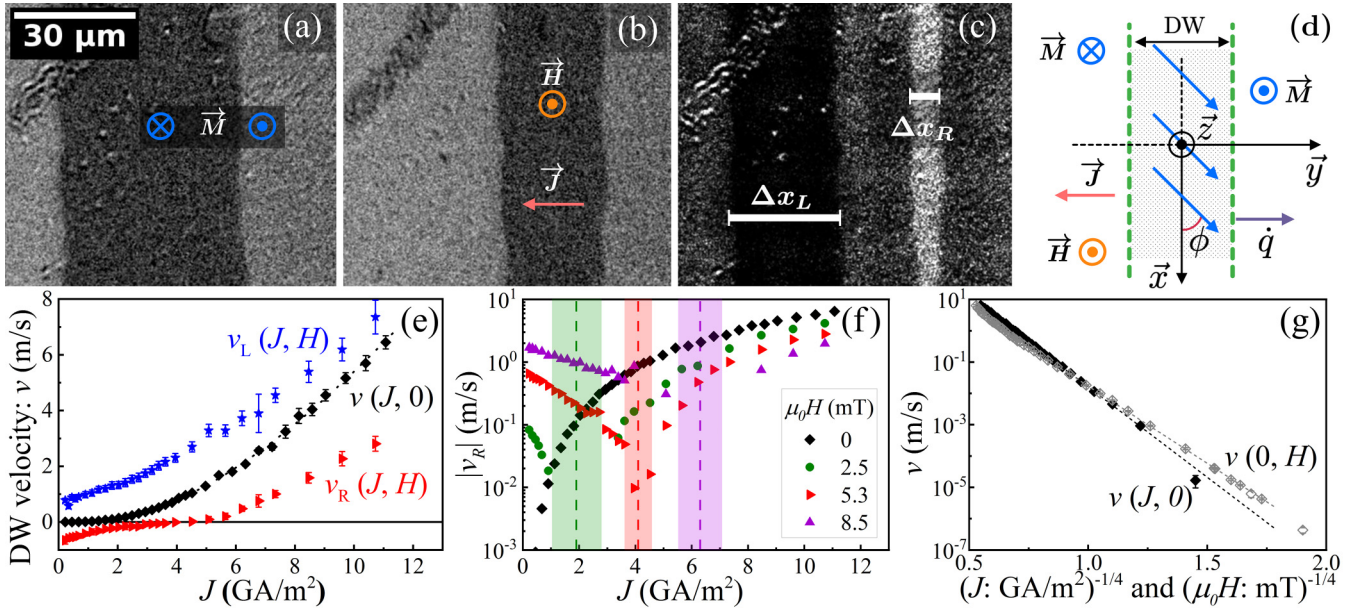
FIG. 1. Phenomenology of domain-wall dynamics. (a)–(c) Displacement of magnetic domain walls produced by simultaneous magnetic-field and current pulses and observed by magneto-optical Kerr effect microscopy. In (a) and (b), the two gray levels correspond to opposite magnetization directions $\vec{M}$, perpendicular to the film. The direction of current density $\vec{J} = -J\hat{y}$ (with $J > 0$) and magnetic field $\mu_0\vec{H} = \mu_0H\hat{z}$ (with $H > 0$) are indicated by arrows in (b). (a) Initial state with three domains separated by two DWs perpendicular to $\vec{J}$. (b) Same DWs after 10 simultaneous current and field pulses of amplitudes $J = 4.5$ GA/m^2 and $\mu_0H = 2.1$ mT and duration $\Delta t = 1.4$ μs. (c) Subtraction of image (a) from (b) enlightening the different mean displacements of the left (Δx_L) and right (Δx_R) DWs. (d) Diagram of a DW magnetic texture, showing in particular the magnetization tilting angle ϕ at the DW center. (e) Velocities versus current density J of the left [$v_L(J, H)$] and right [$v_R(J, H)$] DWs for a finite ($\mu_0H = 5.3$ mT) and a zero [$v(J, 0) = v_L(J, 0) = v_R(J, 0)$] applied magnetic field. (f) Absolute value of $v_R(J, H)$ versus J for different values of μ_0H. The semilog plot emphasizes the drop down of velocity. The vertical dashed lines indicate the values of current density J_c at the compensation condition where the velocity vanishes and the colored shaded surface areas correspond to the associated uncertainties. (g) Independent field [$v(0, H)$] and current [$v(J, 0)$] driven DW velocity in semilog scale versus $(\mu_0H)^{-1/4}$ and $J^{-1/4}$, respectively, evidencing a common scaling creep behavior. All the experiments are performed at $T = 55$ K.

asymmetry with respect to J_c, which enlightens the role played by adiabatic STT on the DW magnetic texture and creep motion, as discussed later.

III. NONADIABATIC SPIN-TRANSFER TORQUE AND DOMAIN-WALL DYNAMICS

A. Compensation between field and current

In order to discuss the compensation between magnetic field and current, we have measured systematically the values of J_c corresponding to the zero crossing of DW velocity ($|v_R| \rightarrow 0$) for a set of fixed applied magnetic field values μ_0H and different temperatures close to T_C. The results are reported in Fig. 2 for the temperature range $T/T_C > 0.8$. As it can be observed, the data cover an order of magnitude in magnetic field values ($0.8 < \mu_0H < 9$ mT) and collapse onto a single master curve. Over this field range, μ_0H is found to be essentially proportional to J_c, with a slope $\mu_0H/J_c = 1.3 \pm 0.2$ mT/(GA/m^2). Moreover, as discussed next, the single slope also strongly suggests that the DW texture remains in the same magnetic state over the whole explored magnetic field range. Note that our analysis of the zero crossing of DW velocity gives direct access to the equivalent torques exerted by magnetic field and current, without any assumption on analogies and differences between the velocity curves proposed in previous works [9,11,13,23,24].

B. Study of the compensation

For the analysis of DW motion, we consider a film of thickness t with infinite lengths in the $\vec{x}$ and $\vec{y}$ direction and a perpendicular magnetic anisotropy K_0. An infinite DW
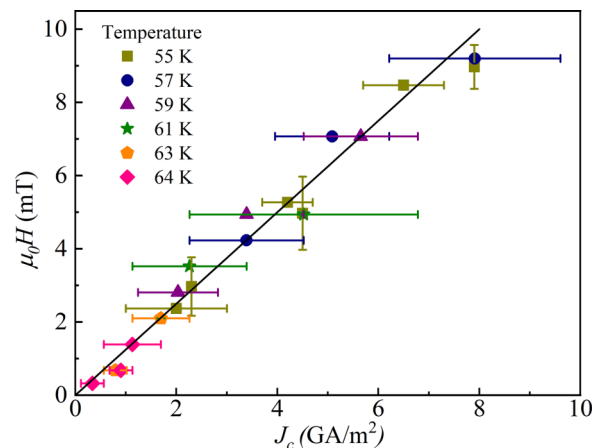

FIG. 2. Current density J_c versus applied magnetic field at the compensation condition corresponding to the zero crossing of DW velocity ($|v_R| \rightarrow 0$). The data obtained for different temperatures close to T_C collapse on a linear variation, whose slope is $\mu_0H/J_c = 1.3 \pm 0.2$ mT/(GA/m^2).

[almost parallel to the x axis; see Fig. 1(d)] separates two domains of saturation magnetization M_s with opposite directions parallel ($+M_s$) and antiparallel ($-M_s$) to $\vec{z}$, respectively. As for the right DW [see Figs. 1(a) and 1(b)], a magnetic field aligned in the direction $\vec{z}$ tends to push the DW along $-y$. A spin polarized current of density $\vec{J} = -J\hat{y}$ (with $J > 0$) is flowing in the direction $-y$ and tends to push the DW along $+y$. The DW position is defined by $q(x)$ and the tilting of magnetization by the angle $\phi(x)$, with $\phi(x) = 0$ corresponding to a Bloch DW. Following Refs. [6,7], the effective potential per unit surface area determining the force exerted on the DW can be written: $\Sigma = \Sigma_q + \Sigma_\phi + \Sigma_{dis}$, where Σ_{dis} is the contribution of the random pinning disorder. The two other terms are

$$\Sigma_q = \frac{\sigma}{2}\left(\frac{dq}{dx}\right)^2 + 2\mu_0 M_s(H - \beta\chi J)q, \quad (1)$$

$$\Sigma_\phi = 2\Delta A\left(\frac{d\phi}{dx}\right)^2 + 2K\Delta\,\sin^2\phi - 2\mu_0 M_s\Delta\chi J\phi. \quad (2)$$

In Eqs. (1) and (2), σ is the DW surface energy and Δ its thickness parameter, A the exchange energy constant, and β the nonadiabatic spin-transfer parameter. $K\,(=\mu_0 M_s H_K/2)$ is the (Bloch-Néel) anisotropy energy of the DW, with $H_K = N_x M_s$ the anisotropy field, and $N_x\,[\approx t/(t + \Delta)]$ is the demagnetizing factor of the DW [30]. The product $\gamma\Delta\chi J$ is the spin drift velocity [4] with

$$\chi = \frac{g\mu_B P}{2|e|\Delta M_s\gamma}, \quad (3)$$

where γ is the gyromagnetic ratio, g the Landé factor, μ_B the Bohr magneton, e the electron charge, and P the spin polarization of current. In Eq. (1), the first term describes the elasticity of the DW and the second term the contribution of the magnetic field and na-STT to the DW drive. The three terms in Eq. (2) reflect the contributions of exchange interaction along the DW, DW Bloch-Néel anisotropy, and a-STT, respectively. Notice here that left and right DWs are related by symmetry and thus are Eqs. (1) and (2): the Zeeman and the a-STT terms for the left DW read $-2\mu_0 M_s(H + \beta\chi J)q$ and $+2\mu_0 M_s\Delta\chi J\phi$, respectively. In the following we focus on the right DW using Eqs. (1) and (2).

For the analysis of compensation between magnetic field and current (see Fig. 2), we start with the so-called q-ϕ model [4], which describes the free motion of a DW ($\Sigma_{dis} = 0$). The DW is assumed to be straight ($dq/dx = 0$) and its magnetization tilt to be homogeneous ($d\phi/dx = 0$). The motion is governed by the Slonczewski equations [4,31]:

$$-\alpha\frac{\dot{q}}{\Delta} + \dot{\phi} = \frac{\gamma}{2\mu_0 M_s}\frac{\delta\Sigma}{\delta q},$$

$$-\frac{\dot{q}}{\Delta} - \alpha\dot{\phi} = \frac{\gamma}{2\mu_0 M_s\Delta}\frac{\delta\Sigma}{\delta\phi}, \quad (4)$$

where α is the Gilbert damping factor, coupling the DW velocity $\dot{q}$ and magnetization precession frequency $\dot{\phi}$ [32]. Inserting Eqs. (1) and (2) into Eqs. (4) and assuming a motion in the steady state ($\dot{\phi} = 0$) leads to the well known result

$$\dot{q} = -\frac{\gamma\Delta}{\alpha}(H - \beta\chi J), \quad (5)$$

$$\alpha\frac{H_K}{2}\sin(2\phi) = H - \beta\chi J + \alpha\chi J, \quad (6)$$

which allows one to examine qualitatively the contribution of a-STT and na-STT to DW motion. At the compensation condition the velocity $\dot{q} \to 0$ [see Eq. (5)], the magnetic field, and na-STT compensate ($H - \beta\chi J = 0$). The proportionality factor $\mu_0 H/J = \mu_0\beta\chi$, where χ is given by Eq. (3), is expected to be constant provided the magnetic state of the DW remains steady. Moreover, for $\dot{q} > 0$, $H - \beta\chi J$ and $\alpha\chi J$ are positive. Both exert torques increasing the magnetization tilt angle $|\phi|$ [see Eq. (6)] and consequently the DW Bloch-Néel anisotropy energy. On the contrary, for $\dot{q} < 0$, the torques exerted by $H - \beta\chi J$ and $\alpha\chi J$ have opposite signs and thus the a-STT tends to maintain a small value of $|\phi|$.

C. DW magnetic state at the compensation

Let us now compare the ratio $\mu_0 H/J = 1.3 \pm 0.2$ mT/(GA/m^2) deduced from Fig. 2 to the prediction at compensation for a steady DW magnetic texture ($\dot{\phi} = 0$). For the ferromagnetic semiconductor (Ga,Mn)As, close to T_C ($0.8 < T/T_C < 1$), the ratio between spin polarization and magnetization is athermal: $P/M_s \approx 0.027(\text{kA m})^{-1}$ [5]. $\Delta = 2.5 \pm 1.0$ nm [33] and $\beta \approx 0.25$ [5] do not vary with temperature. Therefore, the ratio $(\mu_0 H/J)_{st} = \beta\chi = \beta g\mu_B P/(\gamma\Delta 2|e|M_s)$ is expected to be athermal as observed in Fig. 2. The predicted value $(\mu_0 H/J)_{st} = 0.5\text{--}1$ mT/(GA/m^2) ($g = 2$; $\gamma = 1.76\times10^{11}$ Hz/T) is in rather good agreement with experimental results, as already reported in Ref. [10]. In contrast, for the asymptotic precessional state [i.e., a time average of $\sin^2(\phi)$ equal to 0 in Eq. (2)], the predicted ratio $(\mu_0 H/J)_{prec} = (\mu_0 H/J)_{st}[1 + 1/(\beta\alpha)] = 9\text{--}15$ mT/(GA/m^2) is significantly larger than the measurement. This suggests that, at the compensation between magnetic field and na-STT, the DW presents a (fluctuating) magnetic texture remaining close to the steady state.

Moreover, the range ($0.8 < \mu_0 H < 9$ mT) over which the linear variation is observed in Fig. 2 has to be compared to the Walker limit separating the steady and precessional state. Indeed, since $|\sin 2\phi| \leqslant 1$ in Eq. (6), the steady state is expected to occur only over limited ranges of magnetic field and current. At the compensation between field and na-STT ($H - \beta\chi J = 0$), the Walker limit reads $\mu_0 H_w = \mu_0\beta\chi J_w = \alpha\mu_0 H_K/2 \approx 2$ mT (for $T/T_C = 0.9$). Without pinning, the slope $\mu_0 H/J$ should change by about one order of magnitude [$\approx(\mu_0 H/J)_{prec}/(\mu_0 H/J)_{st}$] below and above $\mu_0 H_w$. Therefore, the observation (in Fig. 2) of a constant ratio $\mu_0 H/J$ over the whole range of explored magnetic field indicates that the DW remains in the steady DW state above the Walker limit, which strongly suggests that the pinning disorder impedes the precession of DW magnetization.

IV. ADIABATIC SPIN-TRANSFER TORQUE AND DOMAIN-WALL DYNAMICS

A. Effective driving magnetic field

We now discuss the contribution of a-STT to the creep motion from the velocity curves shown in Figs. 1(e) and 1(f). In the creep regime, the DW velocity is described by [20]:

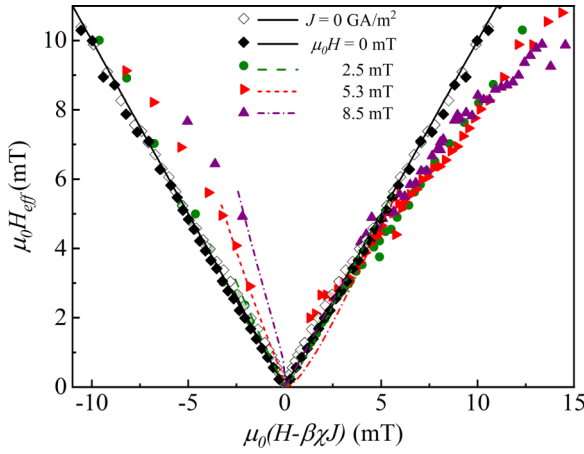$$v(H_{eff}) = v(H_d)\exp\left(-\frac{\Delta E}{k_B T}\right), \quad (7)$$

FIG. 3. Contribution of adiabatic-STT (a-STT) to DW creep motion. Effective magnetic field H_{eff} versus $\mu_0(H - \beta\chi J)$, with $\beta\chi = 1.3$ mT/(GA/m^2) for $J = 0$ GA/m^2 (empty diamonds) and different applied magnetic field values: $\mu_0 H = 0$ mT (filled black diamonds), 2.5 mT (olive circles), 5.3 mT (red right triangles), and 8.5 mT (purple up triangles). The data points are deduced from velocity curves [see Figs. 1(e)–1(g)] and Eq. (8). For $J = 0$ GA/m^2 and $\mu_0 H = 0$ mT, the superposition of curves is compatible with $\mu_0 H_{\text{eff}} = |\mu_0(H - \beta\chi J)|$, which reveals a negligible contribution of a-STT. Increasing the applied magnetic field enlightens a-STT effects: $\mu_0 H_{\text{eff}}$ is enhanced (reduced) for $\mu_0(H - \beta\chi J) < 0$ (>0). The different lines are fits of Eq. (16), using the DW energy of Eq. (12) and are obtained for a single adjustable parameter p (see text).

where $\Delta E = k_B T_d [(H_{\text{eff}}/H_d)^{-\mu} - 1]$ is the effective pinning energy barrier, $\mu = 1/4$ the universal creep exponent, and $k_B T$ the thermal activation energy. In Eq. (7), $k_B T_d$, H_d, and $v(H_d)$ are material dependent parameters characterizing the height of the effective pinning barrier, the depinning threshold, and velocity, respectively. In the following (see Fig. 3), the effective field $H_{\text{eff}}(H, J)$ is assumed to describe both the effect of magnetic field and current on the motion and is used to compare experimental results and theoretical predictions. From Eq. (7), the effective magnetic field can written as a function of the DW velocity $v(H, J)$:

$$H_{\text{eff}}(H, J) = H_d \left[1 - \frac{T}{T_d} \ln \left| \frac{v(H, J)}{v(H_d)} \right| \right]^{-4}. \quad (8)$$

In order to define uniquely the variations of $H_{\text{eff}}(H, J)$ from the velocity curves $v(H, J)$, a set of material dependent parameters was fixed from a fit with Eq. (7) of the velocity curve $v(H, 0)$ [see Fig. 1(g)] obtained for field driven DW motion ($J = 0$). Assuming $v(H_d) = 5.5$ m/s [14], the other pinning parameters are $T_d = 400$ K and $H_d = 13$ mT. For field driven DW motion (with $J = 0$), the effective field is simply $H_{\text{eff}}(H, 0) = |H|$ and corresponds to two straight lines in Fig. 3.

For current driven DW ($H = 0$), the effective field $H_{\text{eff}}(0, J)$ is plotted as a function of $-\mu_0 \beta\chi J$, where we used the value of $\beta\chi$ [$= 1.3$ mT/(GA/m^2)] deduced from the compensation between field and na-STT (see Sec. III). As it can be observed in Fig. 3, the two curves $H_{\text{eff}}(H, 0)$ and $H_{\text{eff}}(0, J)$

are almost perfectly superimposed. This is the expected behavior since the velocity curves $v(H, 0)$ and $v(0, J)$ shown in Fig. 1(g) are close to overlap. The superposition of curves considering only the na-STT indicates that the contribution of a-STT is negligible for current driven DW dynamics with $H = 0$. This is compatible with results reported in Ref. [14], which show that for a DW perpendicular to the current, current and magnetic field driven DW motion follow close universal behaviors for the creep and depinning regimes, corresponding to the quenched Edwards Wilkinson universality class.

For the combined field and current driven DW motion, $\mu_0 H_{\text{eff}}(H, J)$ was deduced from the velocity curves obtained for the right and left DW [see Figs. 1(e) and 1(f)]. The results are plotted in Fig. 3 as a function of $\mu_0(H - \beta\chi J)$ for the right DW and $\mu_0(-H - \beta\chi J)$ for the left DW, for different fixed magnetic field values of $\mu_0 H$. The curves present striking asymmetric features: for the right (left) DW $\mu_0 H_{\text{eff}}$ is increased (reduced) for negative (positive) values of $\mu_0(H - \beta\chi J)$ (i.e., of DW velocity). Close to the compensation $\mu_0(H - \beta\chi J) \approx 0$ mT, raising $\mu_0 H$ increases the necessary current density [$J \approx H/(\beta\chi)$] to achieve the compensation condition ($v \to 0$) and consequently enhances the contribution of a-STT [$\alpha\chi J$; see Eq. (6)]. Therefore, the asymmetric behavior observed in Fig. 3 reflects the contribution to DW creep motion of the a-STT, which may both increase or decrease the effective field [i.e., the effective pinning energy barrier; see Eq. (7)]. This observation is in contradiction with the assumption [6,7] of an a-STT contribution only increasing the pinning energy barrier.

As discussed qualitatively in Sec. III B, assuming steady motion without disorder, for $\dot{q} > 0$ one has that $H - \beta\chi J$ and $\alpha\chi J$ are positive and tend to increase the DW Bloch-Néel anisotropy energy, while for $\dot{q} < 0$, $H - \beta\chi J$ and $\alpha\chi J$ have opposite sign and might change the sign of the energy contribution. With disorder, in the creep regime, increasing the DW energy enhances the pinning barrier heights and reduces the DW velocity. Therefore, the a-STT is expected to reduce DW velocity. On the contrary, for $\dot{q} < 0$, the a-STT tends to maintain a small value of $|\phi|$ and consequently to increase DW velocity. Though this argument is based on the nondisordered case, it qualitatively indicates that the contribution of a-STT to DW dynamics should be asymmetric on both sides of the compensation with a reduced (enhanced) velocity for $\dot{q} > 0$ ($\dot{q} < 0$).

B. Model for the creep motion

In order to analyze more quantitatively the contribution of a-STT and DW texture to creep motion, we use standard scaling arguments [16,34]. The free energy per unit thickness of a DW segment of length L deformed over a distance u [16,35] can be written

$$\delta F = \frac{\sigma}{2} \frac{u^2}{L} - 2\mu_0 M_s |H - \beta\chi J| uL - \delta F_{dis} \pm \Sigma_{\phi DW} L, \quad (9)$$

where the first term is the elastic energy produced by the increase of DW length. The second term is the gain of Zeeman energy due to magnetization reversal; the absolute

value ensures a reduction of the free energy regardless of the sign of $H - \beta\chi J$ (i.e., of the direction of motion). The third term δF_{dis} is the contribution of DW pinning. In addition to those terms commonly used to describe the depinning of an elastic line [16,35], we introduce a term $\Sigma_{\phi DW}L$ associated to the variation of DW magnetic texture with the current. The prefactor $\pm [= \text{sgn}(H - \beta\chi J)]$ of this term accounts for its dependency on the relative direction of current and DW motion (as discussed in the previous section).

Let us now discuss the magnetic texture contribution $\Sigma_{\phi DW}$. Equation (2) describes the variation of magnetization angle along the DW and in particular the structure of Bloch lines [36,37] and their displacement with the current. A theoretical discussion of this effect on the creep motion is beyond the scope of this paper. In the following, we restrict ourselves to the simplest DW texture consisting in a uniform $(d\phi/dx = 0)$ and steady magnetization direction $(\dot\phi = 0)$. For a moving DW whose magnetic texture is at equilibrium one can assume that $\delta\Sigma_\phi/\delta\phi = 0$. Then Eq. (2) leads to

$$\frac{H_K}{2}\sin 2\phi = \chi J. \quad (10)$$

This equation indicates that the a-STT essentially changes the DW magnetization direction. In comparison to Eq. (6), the terms $H - \beta\chi J$ have disappeared since we are considering an equilibrium solution instead of the dynamics as described by the Slonczewski equations. This is effectively equivalent to assuming that there is no coupling between the DW position q and magnetization angle ϕ. (The Euler equations $\delta\Sigma_q/\delta q = 0$ and $\delta\Sigma_\phi/\delta\phi = 0$ were solved separately.) Inserting Eq. (10) into Eq. (2) leads to the energy at equilibrium per unit thickness and length of a DW:

$$\Sigma_{\phi_{st}} = -\tfrac{1}{2}\mu_0 H_K M_s \Delta[\sqrt{1 - h^2} + h \arcsin(h) - 1], \quad (11)$$

where $h = 2\chi J/H_K$. Interestingly, the limit of small tilting angle $[2\phi \approx h;$ see Eq. (10)],

$$\Sigma_{\phi_{st}}(\phi \to 0) = -\frac{\Delta\mu_0}{N_x}(\chi J)^2, \quad (12)$$

remains close to Eq. (11) $[\Sigma_{\phi_{st}}/\Sigma_{\phi_{st}}(\phi \to 0) \leqslant \pi - 2]$ up to the Walker limit $(\phi = \pm\pi/4)$, and therefore enlightens the close scaling of DW anisotropy energy with J^2.

We can now derive the effective magnetic field. With the usual assumption of a DW displacement following the power-law variation $u = u_0(L/L_c)^\zeta$, where $\zeta = 2/3$ is the roughness exponent [14,16] and L_c the so-called collective pinning length, Eq. (9) can be written

$$\delta F(L) = AL^{1/3} - B|H - \beta\chi J|L^{5/3} \pm \Sigma_{\phi_{st}}L, \quad (13)$$

with $A = \sigma u_0^2/(2L_c^{4/3})$ and $B = 2\mu_0 M_s u_0/L_c^{2/3}$. The height of the effective energy barrier is deduced from $\partial\delta F(L = L_{opt})/\partial L = 0$, which yields

$$L_{opt} = \left(\frac{A}{5B}\right)^{3/4}\left(\mp p\Sigma_{\phi_{st}} + \sqrt{\left(p\Sigma_{\phi_{st}}\right)^2 + |H - \beta\chi J|}\right)^{-3/2}. \quad (14)$$

In Eq. (14), we have introduced the constant $p = 3/\sqrt{20AB}$, which depends on the micromagnetic and pinning parameters of the material. Inserting L_{opt} into Eq. (13) leads to the energy barrier

$$\Delta E(H_{\text{eff}}) = \frac{4}{5}\left(\frac{A^5}{5BH_{\text{eff}}}\right)^{1/4}, \quad (15)$$

with the effective field

$$H_{\text{eff}} = |H - \beta\chi J|\frac{[\mp r + \sqrt{1 + r^2}]^{10}}{\left[1 + \tfrac{5}{3}r(r \mp \sqrt{1 + r^2})\right]^4}. \quad (16)$$

The ratio

$$r = \frac{p\Sigma_{\phi_{st}}(J)}{\sqrt{|H - \beta\chi J|}}, \quad (17)$$

present in Eq. (16), suggests an enhanced contribution of a-STT and DW magnetic texture to the creep motion close to compensation $(H - \beta\chi J \to 0)$ between magnetic field and na-STT. Far from the compensation, current driven DW motion is expected to be compatible with the universal behavior of magnetic field driven DW $(\mu = 1/4)$, as observed in Fig. 1, and already reported in Ref. [14]. Equations (15)–(17) predict a deviation from the qEW universal behavior for sufficiently large values of the ratio r.

C. Adiabatic-STT and DW magnetic texture

A quantitative comparison between the predictions for effective field H_{eff} and experimental data is reported in Fig. 3. For the set of curves obtained for different fixed magnetic fields H, we performed a global fit of Eq. (16), including the variation of ratio r [Eq. (17)] and $\Sigma_{\phi_{st}}(\phi \to 0)$ [Eq. (12)]. Note that, since the value of $\beta\chi$ $[= 1.3 \text{ mT}/(\text{GA/m}^2)]$ is fixed, the global fit relies on the single adjustable parameter $p = (2.0 \pm 0.3)\times 10^6 \text{ T}^{-1}(\text{A m})^{-1/2}$. As it can be observed, the prediction presents a rather good agreement with the data close to the compensation (see the dashed lines in Fig. 3). This result demonstrates [see Eq. (10)] that the adiabatic-STT essentially controls the tilt of DW magnetization (and, more generally, the steady DW magnetic texture).

As written previously, the Walker limit would be $\mu_0 H_w \approx 2$ mT without pinning. The fact that data remain in agreement with prediction for the steady DW state for a larger value $(\mu_0 H_{\text{eff}} \approx 4$–5 mT) suggests a contribution of the random pinning potential to maintain a fixed direction of magnetization, as already argued for the compensation. The divergence between experimental findings and theoretical predictions observed at higher effective field suggests a contribution of DW magnetization precession to the creep motion.

It is interesting to assess the variation with micromagnetic and pinning parameters of the a-STT contribution to creep motion from standard scaling arguments. The collective pinning length L_c at depinning $H = H_d$ can be deduced from Eq. (13), assuming $AL_c^{1/3} \sim BHL_c^{5/3}$. Replacing A and B by their expressions, the scaling relation $u_0 \sim \Delta$ yields $L_c \sim [\sigma\Delta/(4\mu_0 M_s H_d)]^{1/2}$ and $p \sim 3/(4\Delta\mu_0 M_s\sqrt{5H_d})$. Moreover, at the compensation $(H - \beta\chi J = 0)$, the contribution of DW magnetic anisotropy should scale with the DW elasticity $\Sigma_{\phi_{st}}L_c \sim AL_c^{1/3}$ [see Eq. (13)], which leads to $\mu_0 H \sim \beta\mu_0\sqrt{M_s H_d N_x}$ Therefore, the contribution of a-STT is expected to be larger and to occur at lower field for material

presenting a low saturation magnetization and weak depinning field.

V. CONCLUSION

Our experimental and theoretical work clarifies the contributions of magnetic field, nonadiabatic-STT, and adiabatic-STT to the creep motion of the domain wall and highlights the interplay between domain walls' magnetic texture and adiabatic-STT.

For the effective pinning barrier height, the magnetic field and na-STT play a similar role. The a-STT introduces a new contribution proportional to the square of current density, which is associated to domain-wall anisotropy. Its sign is positive (negative) when the a-STT contributes to increase (decrease) the domain-wall anisotropy energy and its magnitude is large only close to the compensation between magnetic field and na-STT.

Moreover, the creep motion is found to be closely related to the state of the magnetic texture. Close to the compensation, the magnetic texture corresponds to a quasisteady state with magnetization tilt angle fluctuating around a mean angle

controlled by the a-STT. The data are compatible with the steady state well above the Walker limit predicted for a free DW, which strongly suggests that the random pinning potential depends on DW magnetic texture. Above the Walker limit, the magnetic texture is expected to present more complex behaviors with probably nucleation and motion of Bloch lines, which should be particularly interesting to study.

Implications for the creep motion of interfaces presenting universal behaviors are important since we show that the internal degree of freedom of an elastic interface (the magnetic texture of DW) produces deviation from the prediction of the qEW universality class.

[1] S. S. P. Parkin and S.-H. Yang, Memory on the racetrack, Nat. Nanotechnol. **10**, 195 (2015).

[2] J. Grollier, D. Querlioz, K. Y. Camsari, K. Everschor-Sitte, S. Fukami, and M. D. Stiles, Neuromorphic spintronics, Nat. Electron. **3**, 360 (2020).

[3] S. Zhang and Z. Li, Roles of nonequilibrium conduction electrons on the magnetization dynamics of ferromagnets, Phys. Rev. Lett. **93**, 127204 (2004).

[4] A. Thiaville, Y. Nakatani, J. Miltat, and Y. Suzuki, Micromagnetic understanding of current-driven domain wall motion in patterned nanowires, Europhys. Lett. **69**, 990 (2005).

[5] J. Curiale, A. Lemaître, C. Ulysse, G. Faini, and V. Jeudy, Spin drift velocity, polarization, and current-driven domain-wall motion in (Ga,Mn)(As,P), Phys. Rev. Lett. **108**, 076604 (2012).

[6] R. A. Duine and C. M. Smith, Creep of current-driven domain-wall lines: Effects of intrinsic versus extrinsic pinning, Phys. Rev. B **77**, 094434 (2008).

[7] J. Ryu, S.-B. Choe, and H.-W. Lee, Magnetic domain-wall motion in a nanowire: Depinning and creep, Phys. Rev. B **84**, 075469 (2011).

[8] M. H. Jin, L. Xiong, N. J. Zhou, B. Zheng, and T. J. Zhou, Universality classes of the domain-wall creep motion driven by spin-transfer torques, Phys. Rev. E **103**, 062119 (2021).

[9] M. Yamanouchi, J. Ieda, F. Matsukura, S. E. Barnes, S. Maekawa, and H. Ohno, Universality classes for domain wall motion in the ferromagnetic semiconductor (Ga,Mn)As, Science **317**, 1726 (2007).

[10] J.-P. Adam, N. Vernier, J. Ferré, A. Thiaville, V. Jeudy, A. Lemaître, L. Thevenard, and G. Faini, Nonadiabatic spin-transfer torque in (Ga,Mn)As with perpendicular anisotropy, Phys. Rev. B **80**, 193204 (2009).

[11] J.-C. Lee, K.-J. Kim, J. Ryu, K.-W. Moon, S.-J. Yun, G.-H. Gim, K.-S. Lee, K.-H. Shin, H.-W. Lee, and S.-B. Choe, Universality classes of magnetic domain wall motion, Phys. Rev. Lett. **107**, 067201 (2011).

[12] K.-W. Moon, D.-H. Kim, S.-C. Yoo, C.-G. Cho, S. Hwang, B. Kahng, B.-C. Min, K.-H. Shin, and S.-B. Choe, Distinct universality classes of domain wall roughness in two-dimensional Pt/Co/Pt films, Phys. Rev. Lett. **110**, 139902 (2013).

[13] S. Dutta Gupta, S. Fukami, C. Zhang, H. Sato, M. Yamanouchi, F. Matsukura, and H. Ohno, Adiabatic spin-transfer-torque-induced domain wall creep in a magnetic metal, Nat. Phys. **12**, 333 (2016).

[14] R. Díaz Pardo, N. Moisan, L. J. Albornoz, A. Lemaître, J. Curiale, and V. Jeudy, Common universal behavior of magnetic domain walls driven by spin-polarized electrical current and magnetic field, Phys. Rev. B **100**, 184420 (2019).

[15] P. Chauve, T. Giamarchi, and P. Le Doussal, Creep and depinning in disordered media, Phys. Rev. B **62**, 6241 (2000).

[16] S. Lemerle, J. Ferré, C. Chappert, V. Mathet, T. Giamarchi, and P. Le Doussal, Domain wall creep in an Ising ultrathin magnetic film, Phys. Rev. Lett. **80**, 849 (1998).

[17] E. Agoritsas, V. Lecomte, and T. Giamarchi, Disordered elastic systems and one-dimensional interfaces, Phys. B: Condens. Matter **407**, 1725 (2012).

[18] W. Savero Torres, R. Díaz Pardo, S. Bustingorry, A. B. Kolton, A. Lemaître, and V. Jeudy, Universal dimensional crossover of domain wall dynamics in ferromagnetic films, Phys. Rev. B **99**, 201201(R) (2019).

[19] L. J. Albornoz, P. C. Guruciaga, V. Jeudy, J. Curiale, and S. Bustingorry, Domain-wall roughness in GdFeCo thin films: Crossover length scales and roughness exponents, Phys. Rev. B **104**, 024203 (2021).

[20] V. Jeudy, A. Mougin, S. Bustingorry, W. Savero Torres, J. Gorchon, A. B. Kolton, A. Lemaître, and J.-P. Jamet, Universal

pinning energy barrier for driven domain walls in thin ferromagnetic films, Phys. Rev. Lett. **117**, 057201 (2016).

[21] S. F. Edwards and D. R. Wilkinson, The surface statistics of a granular aggregate, Proc. R. Soc. A **381**, 17 (1982).

[22] O. Boulle, J. Kimling, P. Warnicke, M. Kläui, U. Rüdiger, G. Malinowski, H. J. M. Swagten, B. Koopmans, C. Ulysse, and G. Faini, Nonadiabatic spin transfer torque in high anisotropy magnetic nanowires with narrow domain walls, Phys. Rev. Lett. **101**, 216601 (2008).

[23] L. San Emeterio Alvarez, K.-Y. Wang, S. Lepadatu, S. Landi, S. J. Bending, and C. H. Marrows, Spin-transfer-torque-assisted domain-wall creep in a Co/Pt multilayer wire, Phys. Rev. Lett. **104**, 137205 (2010).

[24] E. Haltz, J. Sampaio, R. Weil, Y. Dumont, and A. Mougin, Strong current actions on ferrimagnetic domain walls in the creep regime, Phys. Rev. B **99**, 104413 (2019).

[25] L. Herrera Diez, V. Jeudy, G. Durin, A. Casiraghi, Y. T. Liu, M. Voto, G. Agnus, D. Bouville, L. Vila, J. Langer, B. Ocker, L. Lopez-Diaz, and D. Ravelosona, Wire edge dependent magnetic domain wall creep, Phys. Rev. B **98**, 054417 (2018).

[26] V. Lecomte, S. E. Barnes, J.-P. Eckmann, and T. Giamarchi, Depinning of domain walls with an internal degree of freedom, Phys. Rev. B **80**, 054413 (2009).

[27] T. Niazi, M. Cormier, D. Lucot, L. Largeau, V. Jeudy, J. Cibert, and A. Lemaître, Electric-field control of the magnetic anisotropy in an ultrathin (Ga,Mn)As/(Ga,Mn)(As,P) bilayer, Appl. Phys. Lett. **102**, 122403 (2013).

[28] J. Curiale, A. Lemaître, G. Faini, and V. Jeudy, Track heating study for current-induced domain wall motion experiments, Appl. Phys. Lett. **97**, 243505 (2010).

[29] J. Curiale, A. Lemaître, T. Niazi, G. Faini, and V. Jeudy, Joule heating and current-induced domain wall motion, J. Appl. Phys. **112**, 103922 (2012).

[30] A. Mougin, M. Cormier, J. P. Adam, P. J. Metaxas, and J. Ferré, Domain wall mobility, stability and Walker breakdown in magnetic nanowires, Europhys. Lett. **78**, 57007 (2007).

[31] J. C. Slonczewski, Dynamics of magnetic domain walls, in *AIP Conf. Proc. No. 5* (AIP, New York, 1972), p. 170.

[32] The proper equations for the left DW are obtained by symmetry using $\dot{q} \rightarrow -\dot{q}$, $J \rightarrow -J$, and $\phi \rightarrow \phi + \pi$.

[33] A. Dourlat, V. Jeudy, A. Lemaître, and C. Gourdon, Field-driven domain-wall dynamics in (Ga,Mn)As films with perpendicular anisotropy, Phys. Rev. B **78**, 161303(R) (2008).

[34] E. Agoritsas, V. Lecomte, and T. Giamarchi, Static fluctuations of a thick one-dimensional interface in the 1+1 directed polymer formulation, Phys. Rev. E **87**, 042406 (2013).

[35] D. M. F. Hartmann, R. A. Duine, M. J. Meijer, H. J. M. Swagten, and R. Lavrijsen, Creep of chiral domain walls, Phys. Rev. B **100**, 094417 (2019).

[36] M. Büttiker and R. Landauer, Nucleation theory of overdamped soliton motion, Phys. Rev. A **23**, 1397 (1981).

[37] A. Malozemoff and J. Slonczewski, *Magnetic Domain Walls in Bubble Materials: Advances in Materials and Device Research* (Academic Press, New York, 2016), Vol. 1.